Journal of Physics and Its Applications

Journal homepage : https://ejournal2.undip.ac.id/index.php/jpa/index

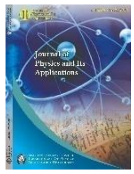

Treatment Dose Delivery Verification using Thimble Chamber and IMRT Phantom

Muhammad Asif[1], Aasia Razzaq[2], Nauman Amjid[2], Tariq Siddique[3], Habib Ahmad[1], Shoab Shah[1], and Javaid Ali[1*]

[1]Swat Institute of Nuclear Medicine, Oncology & Radiotherapy (SINOR), Saidu Sharif Swat, KPK, Pakistan
[2]Institute of Nuclear Medicine and Oncology Lahore (INMOL), Lahore, Punjab, Pakistan
[3]Pakistan Institute of Engineering and Applied Sciences (PIEAS), Islamabad, Pakistan

**Corresponding author: javaidalitarakai@gmail.com*

A R T I C L E I N F O

Article history:
Received: 14 March 2026
Accepted: 20 August 2026
Available online: 31 August 2026

Keywords:
IMRT
Dose verification
Radiotherapy
Ion chamber

ABSTRACT

In external beam radiotherapy, over radiation dose results in severe side-effects, but under radiation dose decreases the probability of treatment for cancer patients. The purpose of the article was to verify treatment dose delivery in radiotherapy of the cancer patients using single point dose verification method. Computed tomography (CT) simulation of intensity-modulated radiation therapy (IMRT) phantom with slot-in ion chamber was done. The IMRT phantom was set on the treatment table of LINAC (Siemens) with FC65-P Farmer type thimble chamber for radiation dose measurement. Different plans were prepared on prowess panther treatment planning system (TPS) using CT images of IMRT Phantom. The monitor units (MU) and doses were calculated for both photon algorithms i.e. Collapsed Cone Convolution Superposition (CCCS) and Fast Photon (FP) algorithms. The calculations for treatment dose verification were done for both 6MV and 15MV energies produced by LINAC (Siemens) at central axis as well as off axis beams. The percentage difference between the measured and calculated dose was less than 1% except for those plans which have greater number of posterior beams. These percentage errors were slightly greater than 1% but well within international recommended limits of ±3% as per ICRU and AAPM. The percentage error in radiotherapy treatment delivery within limit confirms accurate radiotherapy treatment dose delivery with LINAC at the institute. The couch attenuation correction factor while calculating dose on treatment planning system.

1. Introduction

Radiotherapy is a useful technique for treatment of tumor [1]. It is the most frequently used and successful treatment modality after surgery. It is used in more than half of all the cancer patients [2]. The purpose of radiotherapy is to deliver optimum radiation dose to cancer cells and spare organs at risk (OARs), [3-5] which is the prime responsibility of medical physicist. About 60% of all cancer patients after being diagnosed do not have metastatic conditions which can be considered curable. About one third of these cannot be cured because radiotherapy fails to control tumor growth [2]. Therefore treatment verification in radiotherapy of the cancer patients need to be strictly authenticated before radiation delivery [1]. In radiotherapy treatment dose delivery verification of the cancer patients, it is assured that volume of interest (VOI) is treating as it is planned and it is also verified that the radiation dose is delivered accurately at the right place [6]. Different new modalities like three dimensional conformal radiotherapy (3D-CRT), intensity modulated radiotherapy (IMRT), image-guided radiotherapy (IGRT), stereotactic radiotherapy, and particle therapy have been developed [7] in last decades. However, it is not assured that the new modalities are always considered with best results than well tested conventional radiotherapy, in developing countries. Its superiority entirely rests on how much accurate the planning target volume (PTV) is and how dose distribution is with a potential of achieving very good results [8]. Clinical radiation therapy process is complex and involves many steps. This process starts with diagnosis on the basis of CT, MRI, SPECT, PET etc. and then decision for radiation therapy is made by clinical oncologists. Treatment planning (TP) plays an important role in radiotherapy of cancer patients [6]. TP in radiotherapy is done using this anatomical information which is further assessed by analyzing dose volume histograms [9]. After treatment plans evaluation, quality assurance for treatment plan is performed. For 3D-CRT treatment plan, independent monitor units (MU) verification method, manually or computerized, is commonly used. We can also verify treatment plans by performing real time measurements using different dosimeters. MU calculation softwares are based on physical effects which are handled and accurately described by independent set of algorithms [10]. It is very important to have high accuracy in TP of cancer patients in radiotherapy. Therefore a detailed and scheduled quality assurance program (QAP) is necessary to made in every cancer hospital in order to authenticate the treatment dose delivery in treatment planning of radiotherapy cancer patients [6]. Cylindrical ionization chambers are used for point-dose measurements in megavoltage photon radiation therapy because of their excellent stability, linear response to absorbed dose, small directional dependence and especially for the beam-quality response independence [11]. The purpose of the study is to verify treatment delivery of dose in radiotherapy of the cancer patients using single point dose verification method. Also to compare the measured doses with the doses calculated by the Prowess TPS for both CCCS and FP algorithms, for 6MV and 15MV photon energies produced by LINAC (Siemens) at central axis as well as off axis beams.

2. Methods

The materials being used were IMRT phantom, Toshiba Aquilion 16 CT scanner, prowess panther TPS, ONCOR impression linear accelerator (LINAC) of Siemens, FC65-P farmer type thimble chamber and dose 1 electrometer [11]. The complete size of the phantom was 33 cm (L) x 36 cm (W) x 18 cm (H). IMRT phantom consisted of head and neck phantom, two lateral scattering bodies and the torso phantom. The outer dimensions of head and neck phantom were 18 cm x 18 cm x 18 cm which consisted of 16 standard distance plates and 4 compensation plates. Here films could be inserted and also had auxiliary inserts for ion chambers which was one of the concerns of this article. Two lateral scattering bodies which could be mounted on all sides of the cubic phantom complete it to an anthropomorphic shape.

The torso phantom part of the complete phantom consisted of 15 oval shaped slabs having 1 cm thickness. The base plate gave additional security to the phantom. It helped in transportation and lifting of the phantom and also helped to align the phantom correctly during CT or using it under Linac[12]. The IMRT phantom was assembled and farmer chamber was inserted into the slot of the phantom, and then it was taken for the CT simulation. The CT data was then transferred to the prowess TPS through DICOM interface where different plans were prepared for both 6MV and 15MV photon beams. MU were calculated using both FP and CCCS algorithms [6]. The reference point for dose measurement and center of the chamber was located with the help of fiducial markers. The whole data was taken for both central axis and off axis (3 cm distance from center of field having size 10 x 10cm^2) in the experimental set-up as shown in the Fig. 1.

Fig. 1: Experimental set-up for taking the point doses.

Before verification of the mentioned plans correction factors for ion chamber, electrometer and temperature pressure were calculated to rule out the effect of ion recombination, electrometer and temperature pressure. This was done with help of the following steps.

(1) Set gantry angle to zero and SAD = 100cm at the axis of the chamber.
(2) Field size of 10 x 10cm2 was opened with 6MV photon energy.
(3) Applied voltage to farmer chamber was 300V through electrometer.
(4) Delivered 300 MU and measured charge using electrometer.
(5) Reversed the applied voltage to the chamber and set -300V.
(6) Delivered 300 MU and measured the charge.
(7) Adjusted voltage to 150V and again measured the charge by delivering 300 MU.

The gantry angles and MU as calculated by prowess panther TPS using CCCS algorithm were set for different conventional 3D-CRT plans like single field (AP), parallel opposed fields (AP/PA), box fields, four fields oblique, one anterior & two oblique fields, one anterior & two lateral fields, one posterior & two oblique fields and inverted Y-field for 6MV photon beam. All the plans were prepared at TPS as shown in Fig. 2. Before verification of the mentioned plans correction factors for ion chamber, electrometer and temperature pressure were calculated to rule out the effect of ion recombination, electrometer and temperature pressure by the following formulae [13].

$$K_s = \frac{(V_1/V_2)^2 - 1}{(V_1/V_2)^2 - \frac{M1}{M2}} \quad (1)$$

$$K_{pol} = \frac{|M_+| + |M_-|}{2M} \quad (2)$$

$$K_{Tp} = \frac{273.2 + T}{273.2 + T_0} \times \frac{P}{P_0} \quad (3)$$

The charge was measured with an electrometer. The correction factors (Ks, Kpol, K_{TP}) and calibration factor $N_{D,W}$ were applied to convert charge into dose (cGy). For each average value of measured charge (nC) / Mean Measured Dose (cGy) three readings were taken. Point dose was measured for both central and off axis by using equation (4). Calibrated Thermometer, barometer, FC65-P farmer type thimble chamber from SSDL, SSDL, PINSTECH, Islamabad Pakistan were used in these calculations.

$$Dose\ (cGy) = Measured\ charge\ (nC) \times N_{D,w}\ (cGy/nC) \times K_s \times K_{p0l} \times K_{TP} \quad (4)$$

In Equation-4, $N_{D,W}$ is 4.788 (cGy/nC) and it was provided by SSDL, PINSTECH, Islamabad Pakistan. Finally, the percent errors were evaluated by comparing point doses with the doses calculated by the TPS by using equation-5 [6, 14, 15].

$$\%E = \frac{D_{ref} - D_m}{D_{ref}} * 100\% \quad (5)$$

Similar steps were followed when FP algorithm was used but here physical wedges were used unlike CCCS algorithm, in which virtual wedges were used. The whole procedure was also repeated for 15MV beam for both central axis & off axis and for both algorithms.

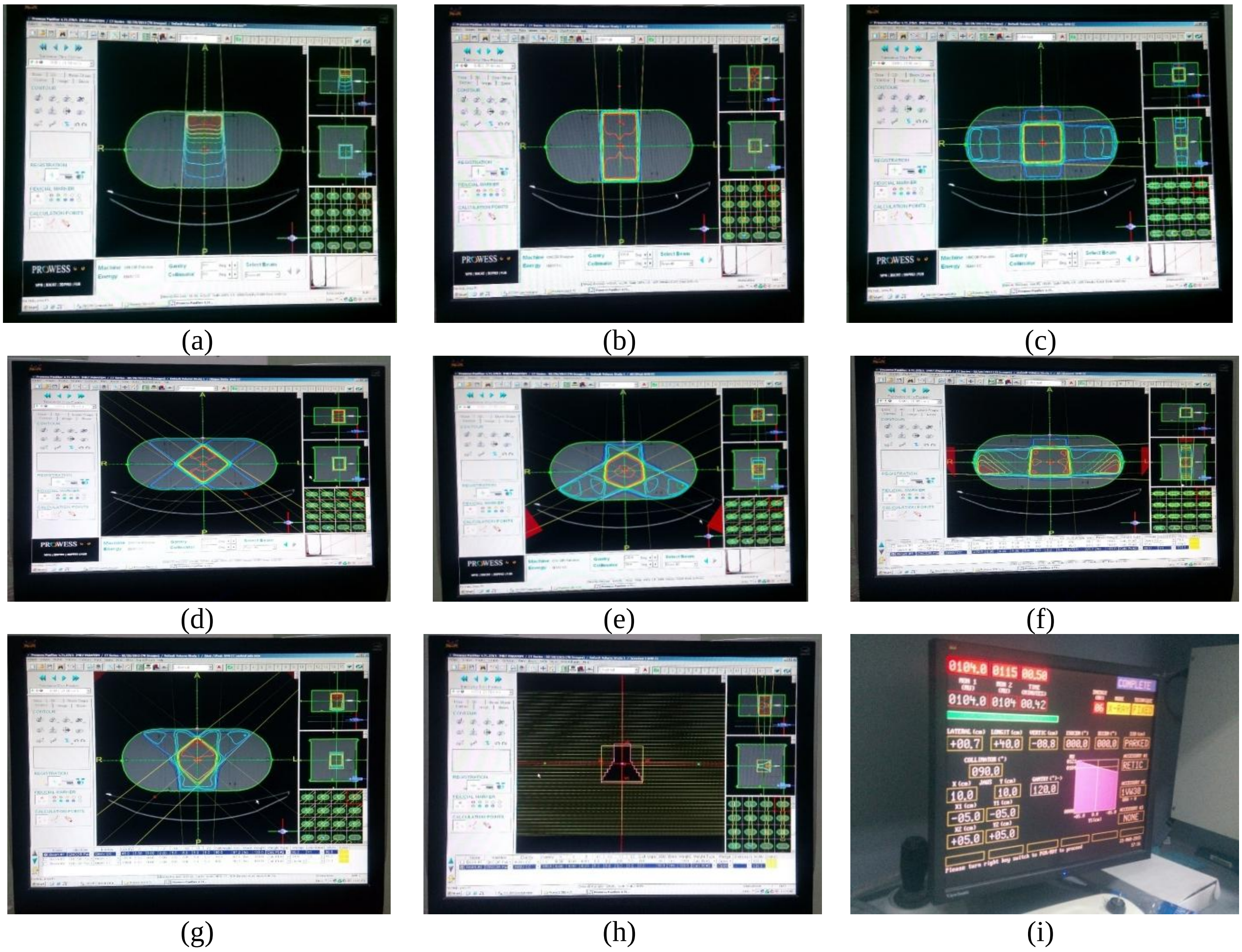

Fig. 2: (a) Single field (b) two fields AP/PA (c) Box fields (d) four oblique fields (e) one anterior two posterior oblique beams (f) one anterior two lateral beams (g) one posterior two anterior oblique beams (h) inverted Y field (i) console reading (Courtesy INMOL).

Table 1: Measured versus CCCS & FP calculated dose for 6MV photon beam.

	Wedge		CCCS	FP
	NIL	Mean Measured Dose (cGy)	175.61	179.44
Single Field	NIL	TPS Dose (cGy)	176.76	178.20
	NIL	% Error	0.65 %	-0.69 %
	NIL	Mean Measured Dose (cGy)	98.96	99.36
AP/PA	NIL	TPS Dose (cGy)	100	100
	NIL	% Error	1.04 %	0.64%
4 field box	NIL	Mean Measured Dose (cGy)	49.87	50.07
	NIL	TPS Dose (cGy)	50	50
	NIL	% Error	0.26%	-0.14%
	NIL	Mean Measured Dose (cGy)	49.52	49.50
4 field oblique	NIL	TPS Dose (cGy)	50	50
	NIL	% Error	0.96%	1.00%
1Ant. 2Post. oblique	NIL	Mean Measured Dose (cGy)	65.69	65.97
	1VW30/4RW30M	TPS Dose (cGy)	66.67	66.67
	2VW30/3RW30M	% Error	1.47%	1.05%
1Ant. 2lateral	NIL	Mean Measured Dose (cGy)	66.75	67.32
	2VW30/3RW30M	TPS Dose (cGy)	66.67	66.67
	2VW30/4RW30M	% Error	-0.12%	-0.97%
Inverted Y	NIL	Mean Measured Dose (cGy)	99.29	98.93
	NIL	TPS Dose (cGy)	100	100
	NIL	% Error	0.71%	1.07%
1 Post. 2 Anterior oblique	NIL	Mean Measured Dose (cGy)	65.97	66.46
	2VW30/3RW30	TPS Dose (cGy)	66.67	66.67
	1VW30/4RW30	% Error	1.05%	0.31%

Table 2: Measured versus CCCS & FP calculated dose for 15MV photon beam.

	Wedge		CCCS	FP
Single Field	NIL	Mean Measured Dose (cGy)	198.00	190.79
	NIL	TPS Dose (cGy)	195.42	191.71
	NIL	% Error	-1.32%	0.48%
AP/PA	NIL	Mean Measured Dose (cGy)	98.98	99.01
	NIL	TPS Dose (cGy)	100.00	100.00
	NIL	% Error	1.02%	0.99%
4 field box	NIL	Mean Measured Dose (cGy)	49.94	49.98
	NIL	TPS Dose (cGy)	50.00	50.00
	NIL	% Error	0.12%	0.04%
4 field oblique	NIL	Mean Measured Dose (cGy)	49.32	49.47
	NIL	TPS Dose (cGy)	50.00	50.00
	NIL	% Error	1.36%	1.06%
1Ant. 2Post. oblique	NIL	Mean Measured Dose (cGy)	65.91	65.93
	1VW30/4RW30M	TPS Dose (cGy)	66.67	66.67
	2VW30/3RW30M	% Error	1.14%	1.11%
1Ant. 2lateral	NIL	Mean Measured Dose (cGy)	66.90	66.58
	2VW30/3RW30M	TPS Dose (cGy)	66.67	66.67
	2VW30/4RW30M	% Error	-0.34%	0.13%
Inverted Y	NIL	Mean Measured Dose (cGy)	98.66	100.00
	NIL	TPS Dose (cGy)	100	100.00
	NIL	% Error	1.34%	0.00%
1 Post. 2 Anterior oblique	NIL	Mean Measured Dose (cGy)	66.09	66.07
	2VW30/3RW30	TPS Dose (cGy)	66.67	66.67
	1VW30/4RW30	% Error	0.87%	0.90%

Table 3: Measured vs CCCS and FP calculated dose for 6MV off axis photon beam.

	Wedge		CCCS	FP
Single Field	NIL	Mean Measured Dose (cGy)	146.10	146.82
	NIL	TPS Dose (cGy)	147.42	147.16
	NIL	% Error	0.90%	0.23%
AP/PA	NIL	Mean Measured Dose (cGy)	99.10	99.61
	NIL	TPS Dose (cGy)	100.00	100.00
	NIL	% Error	0.90%	0.39%
4 field box	NIL	Mean Measured Dose (cGy)	49.72	50.00
	NIL	TPS Dose (cGy)	50.00	50.00
	NIL	% Error	0.56%	0.00%
4 field oblique	NIL	Mean Measured Dose (cGy)	49.56	49.65
	NIL	TPS Dose (cGy)	50.00	50.00
	NIL	% Error	0.88%	0.7%
1Ant. 2Post. oblique	NIL	Mean Measured Dose (cGy)	65.70	66.36
	1VW30/4RW30M	TPS Dose (cGy)	66.67	66.67
	2VW30/3RW30M	% Error	1.46%	0.46%
1Ant. 2lateral	NIL	Mean Measured Dose (cGy)	66.84	66.65
	2VW30/3RW30M	TPS Dose (cGy)	66.67	66.67
	2VW30/4RW30M	% Error	-0.25%	0.03%
Inverted Y	NIL	Mean Measured Dose (cGy)	98.83	98.89
	NIL	TPS Dose (cGy)	100.00	100.00
	NIL	% Error	1.17%	1.11%
1 Post. 2 Anterior oblique	NIL	Mean Measured Dose (cGy)	65.95	66.06
	2VW30/3RW30	TPS Dose (cGy)	66.67	66.67
	1VW30/4RW30	% Error	1.08%	0.91%

Table 4: Measured versus CCCS & FP calculated dose for 15MV off axis photon beam.

	Wedges		CCCS	FP
Single Field	NIL	Mean Measured Dose (cGy)	165.62	157.88
	NIL	TPS Dose (cGy)	166.10	158.03
	NIL	% Error	0.29%	0.09%
AP/PA	NIL	Mean Measured Dose (cGy)	99.31	99.71
	NIL	TPS Dose (cGy)	100.00	100.00
	NIL	% Error	0.70%	0.29%
4 field box	NIL	Mean Measured Dose (cGy)	49.87	50.13
	NIL	TPS Dose (cGy)	50.00	50.00
	NIL	% Error	0.26%	-0.26%
4 field oblique	NIL	Mean Measured Dose (cGy)	49.57	49.62
	NIL	TPS Dose (cGy)	50.00	50.00
	NIL	% Error	0.86%	0.76%
1Ant. 2Post. oblique	NIL	Mean Measured Dose (cGy)	65.91	66.13
	1VW30/4RW30M	TPS Dose (cGy)	66.67	66.67
	2VW30/3RW30M	% Error	1.14%	0.81%
1Ant. 2lateral	NIL	Mean Measured Dose (cGy)	66.78	66.76
	2VW30/3RW30M	TPS Dose (cGy)	66.67	66.67
	2VW30/4RW30M	% Error	-0.16%	-0.13%
Inverted Y	NIL	Mean Measured Dose (cGy)	99.74	99.47
	NIL	TPS Dose (cGy)	100.00	100.00
	NIL	% Error	0.26%	0.53%
1 Post. 2 Anterior oblique	NIL	Mean Measured Dose (cGy)	65.87	65.93
	2VW30/3RW30	TPS Dose (cGy)	66.67	66.67
	1VW30/4RW30	% Error	1.20%	1.11%

Table 5: Mean percent errors for different plans, CCCS, FP algorithms and 6 MV & 15 MV photon beams.

Plans	Gantry Angles	Mean % Error, CCCS, 6 MV Photon Beam (central)	Mean %Error, FP, 6 MV Photon Beam (central)	Mean %Error, CCCS , 15 MV Photon Beam (central)	Mean %Error , FP, 15 MV Photon Beam (central)	Mean % Error, CCCS, 6 MV Photon Beam (off-axis)	Mean %Error, FP, 6 MV Photon Beam (off-axis)	Mean %Error, CCCS , 15 MV Photon Beam (off-axis)	Mean %Error , FP, 15 MV Photon Beam (off-axis)
Single Field	0	0.65	-0.69	-1.32	0.48	0.90	0.23	0.29	0.09
AP/PA	0, 180	1.04 (0.20, 1.88)	0.64 (0.02, 1.27)	1.02 (0.58, 1.45)	0.99 (0.43, 1.55)	0.90 (0.23, 1.61)	0.39 (0.21, 0.57)	0.70 (0.23, 1.16)	0.29 (0.03, 0.55)
4 field box	0, 90, 180, 270	0.26 (0.67, -0.70, 1.93, -0.87)	-0.14 (0.60, 1.34, -1.53, -1.00)	0.12 (0.54, -0.66, -0.90, 1.47)	0.04 (0.50, -1.26, -0.30, 1.23)	0.56 (0.94, -0.28, 1.82, -0.28)	0.00 (0.10, -0.85, 1.58, -0.81)	0.26 (0.43, -0.51, 1.31, -0.21)	-0.26 (0.16, -0.92, 0.30, -0.61)
4 field oblique	45, 135, 225, 315	0.96 (0.05, 1.93, 1.81, 0.06)	1.00 (0.43, 1.84, 1.69, 0.07)	1.36 (0.72, 1.83, 2.00, 0.85)	1.06 (0.64, 1.43, 1.46, 0.70)	0.88 (0.47, 1.58, 1.14, 0.30)	0.70 (0.54, 1.14, 0.74, 0.37)	0.86 (0.30, 1.38, 1.45, 0.30)	0.76 (0.27, 1.04, 1.07, 0.64)
1Ant. 2Post. oblique	0, 120, 240	1.47 (0.53, 1.90, 1.95)	1.05 - 0.56, 1.88, 1.85)	1.14 (0.51, 1.48, 1.43)	1.11 (0.48, 1.43, 1.41)	1.46 (0.95, 1.51, 1.91)	0.46 (0.47, 1.53, 0.90)	1.14 (0.35, 1.59, 1.51)	0.81 (0.14, 1.26, 1.03)
1Ant. 2lateral	0, 90, 270	-0.12 (0.51, -0.42, -0.47)	-0.97 (0.61, -1.97, -1.57)	-0.34 (0.80, -0.54, -1.29)	0.13 (0.56, -0.74, 0.61)	-0.25 (1.48, -1.45, -0.79)	0.03 (0.57, -0.26, -0.24)	-0.16 (0.35, -0.59, -0.24)	-0.13 (0.14, -0.36, -0.19,)
Inverted Y	0, 180	0.71 (0.35, 1.07)	1.07 (0.38, 1.75)	1.34 (0.95, 1.73)	0.00 - 1.31, 1.32)	1.17 (0.60, 1.75)	1.11 (0.32, 1.09)	0.26 - 0.31, 0.82)	0.53 (0.05, 1.01)
1 Post. 2 Anterior Oblique	180, 45, 315	1.05 (1.91, 0.25, 0.98)	0.31 (1.84, -0.14, -0.79)	0.87 (1.46, -0.29, 0.78)	0.90 (1.46, 0.75, 0.47)	1.08 (1.89, 0.55, 0.80)	0.91 (1.79, 0.88, 0.07)	1.20 (1.26, 1.53, 0.83)	1.11 (1.69, 0.67, 0.98)

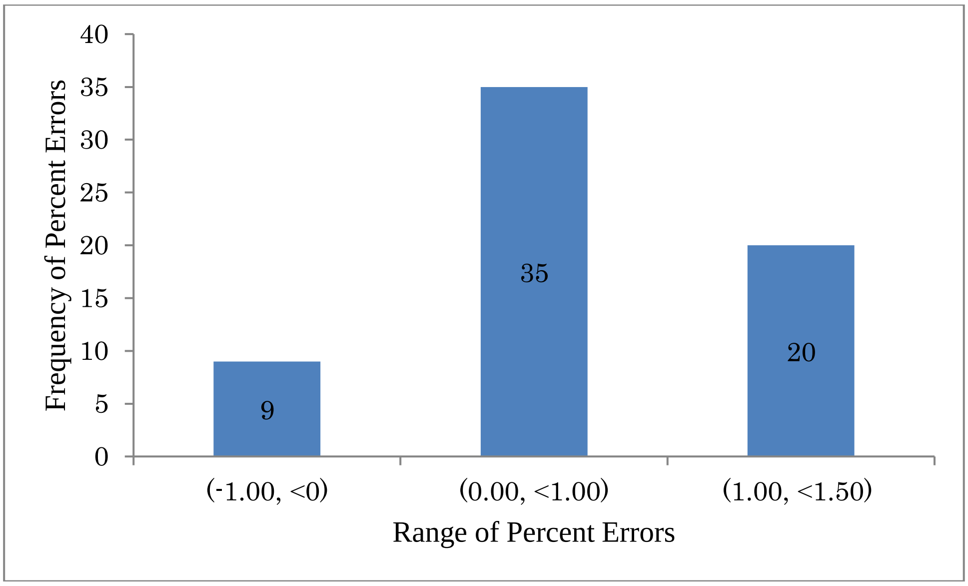

Fig. 3: Frequency of Cumulative % errors of the entire off axis and central axis photon

3. Results and Discussion

The data calculated at central axis and off axis for 6MV & 15MV photon beams for both CCCS and FP algorithms is tabulated in Table-1-4. In taking the data individual beams of different plans, their gantry and collimator angles, type of wedge used, MU calculated by CCCS and PF algorithms, dose calculated by the TPS and dose measured by ion chamber were applied for symmetric field size of 10 x 10cm^2 for the verification of data.

The cumulative percentage errors between the thimble chamber's measured point doses and doses calculated by the TPS for off axis and central axis photon beams are shown in Fig. 3.

The frequency of cumulative percent errors in Fig. 3 is in good agreement with the international permissible limit of ±3.00%. The data verified experimentally for central and off-axis 6 MV and 15 MV photon beams for different gantry angles and anterior (AP) beams are well within permissible limits and have very less percentage error i.e. less than 1% as shown in Tables-1-4. However all posterior (PA) beams have percentage errors relatively greater than 1%, still within ±3 [16] for both 6 MV & 15 MV photons and both CCCS & FP algorithms. Also, the same is within limit of 2 to 5% as suggested for complex geometries [17], as shown in Table-5 (as highlighted).

Table-05 shows that those plans which had greater number of posterior beams have percentage errors slightly greater than 1%, which may be due to couch attenuation [18], improper positioning of active volume of thimble chamber and difference in actual filed setting in taking data experimentally and field for calibration of LINAC. Other reasons for these errors may be that active volume of the thimble chamber (as it is relatively large) may not be precisely located at the position for which calculation of the dose has been done on the Prowess Panther TPS. Also, actual calibration of the linac had been done using water phantom and 40x40cm^2 field size. Table-05 also shows that percent errors are well within acceptable limit of ±3 [16] for both CCCS and FP for all plans and both energies 6 MV 15 MV proving high accuracy of dose delivery with LINAC (Siemens). So, the percent errors in radiotherapy treatment dose verification using thimble chamber are well in agreement with international limit verified accurate radiotherapy treatment dose delivery with LINAC at Institute of Nuclear Medicine and Oncology Lahore (INMOL) Punjab, Pakistan.

4. Conclusion

It was concluded that very small percent errors in radiation treatment delivery confirms good dosimetric agreement between the TPS calculations and point-dose measurements and hence accurate radiotherapy treatment dose delivery with LINAC (Siemens) at the institute. Present study shows the applicability of conventional ionization chamber in 3D-CRT. Also, the couch attenuation lessens the posterior beams' doses, very slightly but should be incorporated while calculating dose on treatment planning system in order to further improve efficacy of radiation treatment delivery. Future work is also needed to compare this simple method with well-established small field dosimeters like diamond detectors.

References

[1] Zhang, J., et al., A method for in vivo treatment verification of IMRT and VMAT based on electronic portal imaging device. Radiation Oncology, 2021. 16: p. 1-15.

[2] Schlegel, W., et al., New Technologies in Radiation Oncology. Journal of Nuclear Medicine, 2008. 49(4): p. 683-684.

[3] Emami, B., Tolerance of normal tissue to therapeutic radiation. Reports of radiotherapy and Oncology, 2013. 1(1): p. 123-7.

[4] Abdollahi, H., et al., Radiomics-guided radiation therapy: opportunities and challenges. Physics in Medicine & Biology, 2022. 67(12): p. 12TR02.

[5] Zhang, W., et al., Real-time, volumetric imaging of radiation dose delivery deep into the liver during cancer treatment. Nature Biotechnology, 2023: p. 1-8.

[6] Singh, S., P. Raina, and O. Gurjar, Point Dose Measurement for Verification of Treatment Planning System using an Indigenous Heterogeneous Pelvis Phantom for Clarkson, Convolution, Superposition, and Fast Superposition Algorithms. Journal of Biomedical Physics & Engineering, 2019. 9(6): p. 613.

[7] Koka, K., et al., Technological advancements in external beam radiation therapy (EBRT): An indispensable tool for cancer treatment. Cancer Management and Research, 2022: p. 1421-1429.
[8] Khan, F.M., The physics of radiation therapy. 2010: Lippincott Williams & Wilkins.
[9] Sharpe, M.B., IAEA Technical Reports Series No. 430: Commissioning and Quality Assurance of Computerized Planning Systems for Radiation Treatment of Cancer. Medical Physics, 2006. 33(2): p. 561-561.
[10] Al Amri, I., et al., Radiotherapy pre-treatment dose validation: A second verification of monitor units (MU) with a commercial software. Journal of medical physics/Association of Medical Physicists of India, 2012. 37(4): p. 235.
[11] Low, D.A., et al., Dosimetry tools and techniques for IMRT. Medical physics, 2011. 38(3): p. 1313-1338.
[12] I'mRT Phantom User's Guide. 2003, IBA Dosimetry: Germany.
[13] TRS, I., 398" Absorbed dose determination in external beam radiotherapy: An international code of practice for dosimetry based on standards of absorbed dose to water. International Atomic Energy Agency, Vienna, 2000.
[14] Ali, J., et al., Estimation of net percent error in radioiodine-131 activity during administration to patients. Pakistan Journal of Nuclear Medicine, 2023. 13(1): p. 20-20.
[15] Ali, J., A.U. Khan, and S. Ali, Theoretical comparison of absorbed dose estimation using dose commitment formula and medical internal radiation dose in radioactive iodine-131 therapy. Pakistan Journal of Nuclear Medicine, 2020. 10(1): p. 1-4.
[16] Bhangle, J.R., V.S. Narayanan, and S.A. Deshpande, Dose linearity and uniformity of Siemens ONCOR impression plus linear accelerator designed for step-and-shoot intensity-modulated radiation therapy. Journal of Medical Physics/Association of Medical Physicists of India, 2007. 32(3): p. 103.
[17] Venselaar, J., H. Welleweerd, and B. Mijnheer, Tolerances for the accuracy of photon beam dose calculations of treatment planning systems. Radiotherapy and oncology, 2001. 60(2): p. 191-201.
[18] Botha, J.J., The evaluation of an algorithmic model, created for the image guided radiotherapy treatment couch for integration into the Pinnacle Treatment Planning System. 2020, Cape Peninsula University of Technology.